AIAA JOURNAL
Vol. 43, No. 10, October 2005

Analysis and Characteristics of Choked Swirling Nozzle Flows

Alon Gany,* Marat Mor,† and Claudio Goldman‡
Technion—Israel Institute of Technology, 32000 Haifa, Israel

A novel analysis is presented of swirling flows in choked nozzles. The one-dimensional compressible flow theory was extended to isentropic axisymmetric swirling flows. The most significant accomplishment of the present model is its ability to treat a general swirl type of any tangential velocity distribution. A choking criterion similar to that of one-dimensional nonswirling flows was introduced. The development of a simplified analytical formulation was shown to ease the solution procedure and to yield good approximations. Model predictions revealed swirl intensity and type effects on Mach number distribution at the throat, indicating a tendency for the axial Mach number to exceed unity at a part of the nozzle throat cross section. The mass flow rate was found to decrease with increasing swirl intensity for fixed stagnation conditions.

Nomenclature

a	=	constant defined in Eq. (18)
a^*	=	speed of sound at Mach number of unity
b	=	constant defined in Eq. (19)
C_m	=	mass flux coefficient
f	=	function describing tangential velocity profile
g	=	function defined in Eq. (9)
h	=	specific stagnation enthalpy
L	=	parameter
M_x, M_θ	=	axial and tangential components of Mach number based on a^*
$\dot{m}$	=	mass flow rate
n	=	power of the solid/free solid-body swirl-type rotation
R_e	=	radius at the wall
r	=	radius; radial coordinate
S	=	swirl number
s	=	specific entropy
T	=	temperature
u	=	axial velocity
$\boldsymbol{u}$	=	velocity vector
w	=	tangential velocity
x	=	axial coordinate
γ	=	specific heat ratio
Δ	=	distance from the centerline
δ	=	function defined in Eq. (16)
ε	=	function defined in Eq. (15)
λ	=	function defined in Eq. (17)
ρ	=	density
ϕ	=	parameter

Subscripts

a	=	nozzle axis
e	=	wall
t	=	nozzle throat
0	=	stagnation conditions
1	=	reference cross section
$*$	=	conditions at Mach number of unity

Received 24 September 2001; accepted for publication 3 February 2005.

*Professor, Lena and Ben Fohrman Chair in Aeronautical Engineering, and Head, Fine Rocket Propulsion Center; gany@tx.technion.ac.il. Associate Fellow AIAA.

†Faculty of Aerospace Engineering; currently Research Associate, Department of Aeronautics and Astronautics, University of Washington, Seattle, WA 98195; mor@aa.washington.edu.

‡Faculty of Aerospace Engineering; currently Engineer, Andersen Consulting, Buenos Aires, Argentina.

I. Introduction

THE objective of this work is to analyze nonviscous choked swirling flows, introducing a theoretical model that can accommodate a general swirl type. Besides the generality of the approach, it uses an explicit choking criterion, and the equations are cast in a compact form to ease the solution of the entire flowfield in the nozzle.

The relatively simple one-dimensional transonic flow becomes much more complex when introducing a tangential velocity component to the flow. Earlier swirling flow models, for example, by Mager,[1] King,[2] Lewellen et al.,[3] and Gillespie and Shearer,[4] were often restricted to the solution of a simple swirl type. Mager[1] presented an approximate solution for a swirling, free vortex, potential flow. One of his conclusions was that at each axial position there is a core zone between the axis and a certain radius, where no flow exists, and hence, it could be represented by zero density. Analysis and solutions for an inviscid free vortex nozzle flow resulting in similar conclusions were also presented in Ref. 4. A simple analytical approach similar to that of Mager[1] treating a swirl type of similar characteristics has been introduced by Cutler and Barnwell,[5] who also conducted experiments of swirling flow through a converging–diverging nozzle. King[2] solved the specific case of a tangential velocity distribution as a solid-body rotation. His solution assumed low swirl intensity throughout the nozzle and given values of Mach number along the axis. Batson and Sforzini[6] noted that the specific swirl types used, because of their simple analytical expressions, may not be adequate representations of actual swirling flows. Lewellen et al.[3] made significant analytical as well as experimental contributions. Their analytical model assumed isentropic flow of a perfect gas, predicting the effects of swirl by expanding the one-dimensional flow theory. The analysis led to two nonlinear ordinary differential equations for Mach number and flow function vs the radial coordinate. The choking radial distribution of the axial Mach number could be found by obtaining the maximum value of flow rate vs the centerline axial Mach number for a fixed nozzle radius. The model was limited to a specific family of swirl types. Lewellen et al.[3] reported that experimental visualization studies revealed no existence of zero- or reverse-flow core in the transonic flow range. Norton et al.[7] added a correction for viscous effects to the inviscid theory. They showed that the inviscid model could yield good agreement with free-vortex test results. However, viscous effects seemed to be more pronounced in the cases of strong forced-vortex nozzle flows associated with high contraction ratios in the nozzle.

Note that, besides analytical models and solutions, three-dimensional codes[8] have been developed using powerful computers, which could give numerical solutions of complex flows.

Swirling flows are of practical significance in different devices, for example, cyclone separators, burners, and spinning rockets.

Theoretical as well as experimental investigations[7,9,10] have often been aimed at different engineering applications. The effect of increased flow resistance with imposing swirl on a choked nozzle flow seems to be of particular interest in rockets, where the purposeful use of swirl to control flow rate and thrust has been analyzed and tested.[11–14]

II. Analytical Model

For a steady and frictionless flow, the equation of motion can be expressed as[15]

$$\nabla h - T\nabla s = \tfrac{1}{2}\nabla|u|^2 - \boldsymbol{u}\cdot\nabla\boldsymbol{u} \tag{1}$$

where h and s are the flow specific stagnation enthalpy and entropy, respectively, and T is the flow temperature. In view of the vector identity

$$\boldsymbol{u}\times(\nabla\times\boldsymbol{u}) = \tfrac{1}{2}\nabla|u|^2 - \boldsymbol{u}\cdot\nabla\boldsymbol{u} \tag{2}$$

Eq. (1) can be rewritten as

$$\boldsymbol{u}\times(\nabla\times\boldsymbol{u}) = \nabla h - T\nabla s \tag{3}$$

Equation (3) is known as the Crocco relation. When isentropic flow of constant stagnation enthalpy is assumed, Eq. (3) becomes

$$\boldsymbol{u}\times(\nabla\times\boldsymbol{u}) = 0 \tag{4}$$

For an axisymmetric flow and a sufficiently gradual change of the nozzle cross section (termed by Gillespie and Shearer[4] quasi-cylindrical nozzle), one can assume that the radial velocity and its derivatives can be neglected. Lewellen et al.[3] as well as Norton et al.[7] used this assumption in their analyses, whereas Batson and Sforzini[6] demonstrated experimentally that the radial velocity component is indeed negligible with respect to the axial and tangential components. Under such conditions, the only nontrivial component of Eq. (4) is

$$\frac{w}{r}\frac{\mathrm{d}}{\mathrm{d}r}(rw) + u\frac{\mathrm{d}u}{\mathrm{d}r} = 0 \tag{5}$$

A swirling flow through a converging–diverging nozzle as well as the corresponding notation are given in Fig. 1. Equation (5) connects the axial and tangential (swirl) components of the velocity (u and w, respectively) at a cross section. Integration of Eq. (5) at a particular section gives

$$u^2 = u_a^2 - 2\int_0^r \frac{w}{\eta}\frac{\mathrm{d}}{\mathrm{d}\eta}(\eta w)\,\mathrm{d}\eta \tag{6}$$

The tangential velocity profile at a cross section is described by the form

$$w = w_e f(r) \tag{7}$$

where $f(r)$ is a general nondimensional function of r and w_e is a constant (equal to the tangential velocity at the nozzle wall) for each specific cross section. The subscript a denotes values at the centerline. In practice, conservation of angular momentum yields wr = constant along a streamline. When a particular cross section, denoted 1, is designated as a reference (Fig. 1) and Eq. (7) is applied, Eq. (6) becomes

$$u_1^2 = u_{a1}^2 - w_{e1}^2 g^2(r_1) \tag{8}$$

where u_{a1} is the axial velocity at the centerline of cross section 1 and $g^2(r_1)$ is defined as follows:

$$g^2(r_1) = 2\int_0^{r_1} \frac{f(\eta)}{\eta}\frac{\mathrm{d}}{\mathrm{d}\eta}[f(\eta)\eta]\,\mathrm{d}\eta \tag{9}$$

In Eq. (8), the term $f^2(R_{e1})$ is missing because, as results from Eq. (7), $f(R_{e1}) = 1$. Note that the conservation of angular momentum along a streamline implies similarity of the tangential velocity profile $f(r)$ at each cross section.

The next step is to determine the axial velocity at the centerline u_{a1}, by applying a geometric criterion $\mathrm{d}R_e/\mathrm{d}x = 0$, characterizing the throat section of a converging–diverging nozzle, where x is the axial coordinate. Because at the throat of a choked (supersonic) converging–diverging nozzle $\mathrm{d}u/\mathrm{d}x \neq 0$, the following expression can be used as a choked nozzle criterion:

$$\frac{\mathrm{d}R_{et}}{\mathrm{d}u_{at}} = 0 \tag{10}$$

where the index t refers to the throat cross section.

Now we need a relation between R_e (nozzle contour) and u_a to make use of this criterion. Conservation of mass along a stream tube of a thickness $\mathrm{d}r$

$$\rho ur\,\mathrm{d}r = \rho_1 u_1 r_1\,\mathrm{d}r_1 \tag{11}$$

where ρ is the flow density, yields an implicit relation between R_e and u_a,

$$R_e^2 = 2\int_0^{R_{e1}} \frac{\rho_1 u_1}{\rho u} r_1\,\mathrm{d}r_1 \tag{12}$$

By the selection of the throat cross section to coincide with the reference cross section 1, Eq. (12) together with the choked nozzle criterion [Eq. (10)] can be solved by a numerical iterative method (referred to as exact solution), yielding the value of u_{a1} for choked conditions.

A simplified solution procedure may yield good approximations in cases involving low swirl intensities. An approximate expression for the isentropic ratio between static and stagnation densities ρ/ρ_0 is particularly useful in the transonic flow zone,

$$\rho/\rho_0 \approx \left\{1 - [(\gamma-1)/(\gamma+1)]\left(M_x^2 + M_\theta^2\right)\right\}^{1/(\gamma-1)} \tag{13}$$

where M_x and M_θ are defined as u/a^* and w/a^*, respectively (close approximations of the axial and tangential Mach numbers in the vicinity of the choked nozzle throat), where a^* is the speed of sound at Mach number of unity.

Using Eq. (13) together with Eqs. (6) and (9) (rewritten in terms of Mach numbers), one obtains

$$\rho M_x/\rho_0 = \lambda^b M_{xa}\left\{1 - \left[\varepsilon^2 - (a/\lambda)\delta^2 M_{xa}^2\right]\right\}^b \sqrt{1-\delta^2} \tag{14}$$

where ε and δ are defined as follows:

$$\varepsilon^2 = (a/\lambda)M_\theta^2 = (a/\lambda)M_{\theta e}^2 f^2 \tag{15}$$

$$\delta^2 = (M_{\theta e}/M_{xa})^2 g^2 \tag{16}$$

$$\lambda = 1 - a\,M_{xa}^2 \tag{17}$$

$$a = (\gamma-1)/(\gamma+1) \tag{18}$$

$$b = 1/(\gamma-1) \tag{19}$$

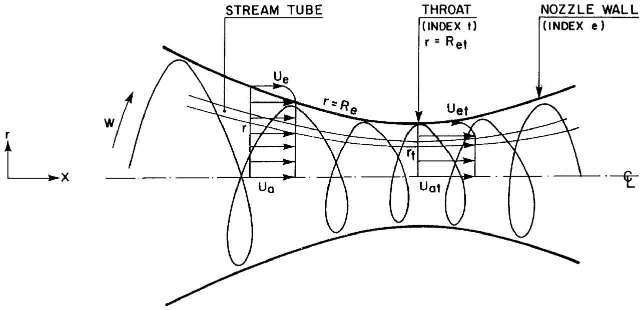

Fig. 1 Swirling flow through a nozzle.

Using Eq. (14), we write Eq. (12) in the following form:

$$\frac{R_e^2}{2} = \left(\frac{R_e}{R_{e1}}\right)^2 \int_0^{R_{e1}} \sqrt{\frac{1-\delta_1^2}{1-\delta^2}} \left\{ \frac{1-\left[\varepsilon_1^2 - (a/\lambda_1)\delta_1^2 M_{xa1}^2\right]}{1-\left[\varepsilon^2 - (a/\lambda)\delta^2 M_{xa}^2\right]} \right\}^b r_1\,\mathrm{d}r_1 \tag{20}$$

where

$$(R_e/R_{e1})^2 = (M_{xa1}/M_{xa})(\lambda_1/\lambda)^b \tag{21}$$

Equation (21) is a relation for the area ratio in the case of nonswirling flow.

If cross section 1 coincides with the throat cross section (indexed t), then substituting Eq. (17) for λ into Eq. (20), differentiating it with respect to M_{xa}, while neglecting the derivatives of ε^2, δ^2, one obtains, by applying the choking criterion from Eq. (10),

$$\frac{M_{xat}^2 - 1}{M_{xat}\lambda_t}\frac{R_{et}^2}{2} - \int_0^{R_{et}} 2\frac{b}{M_{xat}\lambda_t}\frac{1-\lambda_t}{\left[\left(1-\varepsilon_t^2\right)/\delta_t^2 - 1\right]\lambda t + 1} r_t\,\mathrm{d}r_t = 0 \tag{22}$$

The procedure allows very simple and precise approximations for $M_{\theta e}$, as will be presented. Expanding the integrant in Eq. (22) to a series with respect to ε_t^2 and δ_t^2, neglecting the terms of order $\mathcal{O}(\delta_t^6, \varepsilon_t^2\delta_t^4, \varepsilon_t^4\delta_t^2)$ (which contain $M_{\theta et}^6$), and substituting Eqs. (15) and (16), one obtains

$$\frac{M_{xat}^2 - 1}{2}\frac{R_{et}^2}{2} - \frac{1-\lambda_t}{\lambda_t} b \left(\frac{M_{\theta et}}{M_{xat}}\right)^2 \int_0^{R_{et}} \left[g_t^2 + \frac{1-\lambda_t}{\lambda_t}\left(\frac{M_{\theta et}}{M_{xat}}\right)^2 \times \left(g_t^2 f_t^2 - g_t^4\right)\right] r_t\,\mathrm{d}r_t = 0 \tag{23}$$

An approximate value of M_{xat} is obtained by solving Eq. (23). For the nonswirl case ($M_\theta = 0$), Eq. (23) reduces to the area–velocity relation of a one-dimensional compressible flow. In that case, the axial Mach number at the nozzle throat is equal to unity.

One of the important aspects of a swirling flow is the influence of the swirl on the so-called mass flux coefficient C_m, defined by

$$C_m = \dot{m} \big/ \pi R_{et}^2 \rho^* a^* \tag{24}$$

where the asterisk denotes conditions at Mach number of unity.

The effect of C_m is equivalent to the effect of reducing the throat area in a nonswirling flow. When substituted for

$$\dot{m} = \int_A \rho u\,\mathrm{d}A$$

and When the relation in Eq. (14) (at the throat cross section) is used, Eq. (24) can be modified as follows:

$$C_m = \frac{2}{R_{et}^2}\left(\frac{\rho^*}{\rho_0}\right)^{-1} \lambda^b M_{xat} \int_0^{R_{et}} \left[1 - \left(\varepsilon_t^2 - \frac{a}{\lambda_t}\delta_t^2 M_{xat}^2\right)\right]^b \times \sqrt{1-\delta_t^2}\, r_t\,\mathrm{d}r_t \tag{25}$$

When the integrant in Eq. (25) is expanded to a series, similar to the demonstrated procedure [see Eq. (23)] and $(\rho^*/\rho_0)^{-1} = (1-a)^{-b}$ obtained from Eq. (13) is substituted, the following expression for the mass flux coefficient is found:

$$C_m = \frac{2}{R_{et}^2}\left(\frac{\lambda_t}{1-a}\right)^b M_{xat} \int_0^{R_{et}} \sqrt{1 - \left(\frac{M_{\theta et}}{M_{xat}}\right)^2 g_t^2} \times \left[1 - \frac{1-\lambda_t}{\lambda_t}\left(\frac{M_{\theta et}}{M_{xat}}\right)^2 \left(f_t^2 - g_t^2\right)\right]^b r_t\,\mathrm{d}r_t \tag{26}$$

III. Results and Discussion

For the flow characteristics, three specific swirl types of a general form $w = w_e f(r)$ were studied in detail: solid-body-type rotation, $f(r) = (r/R_e)^n$, $n > 0$; free-vortex-type flow, $f(r) = (r/R_e)^n$, $n \le 0$; and an exponential velocity profile,

$$f(r) = \frac{1 - \exp\left[-(r/r_0)^2\right]}{1 - \exp\left[-(R_e/r_0)^2\right]}\frac{R_e}{r}$$

Applying the simplified formulation developed in this study, we found approximate analytical solutions for the tangential Mach number at the wall of the nozzle throat for the different swirl types using Eq. (23). The resulting expressions are presented next. The approximate expressions for the tangential and axial Mach numbers at the nozzle throat for various swirl types of the general form $w = w_e(r/R_e)^n$ are as follows:

For $n > 0$,

$$M_{\theta et} = \sqrt{\frac{\lambda_t}{a}\phi\left(1 - \sqrt{1 - n\frac{M_{xat}^2 - 1}{b\phi}}\right)}, \qquad \phi = n\frac{n + 1/2}{n+1} \tag{27}$$

$$M_{xt}^2 = M_{xat}^2 - M_{\theta et}^2\left(1 + \frac{1}{n}\right)\left(\frac{r_t}{R_{et}}\right)^{2n} \tag{28}$$

Note that in the case of a free-vortex-type flow, the low boundary of the integrals in Eqs. (9) and (23) is changed from zero to Δ_t because of a singularity $r = 0$. Then $M_{x\Delta t}$ is defined as an axial Mach number at a distance Δ_t from the centerline. Here the analysis was done for $\Delta_t \ll R_{et}$. For $n = 0$,

$$M_{\theta et} = \sqrt{\frac{\lambda_t}{a}\phi\left(1 - \sqrt{1 - \frac{1}{2L-1}\frac{M_{x\Delta t}^2 - 1}{b\phi}}\right)}$$

$$\phi = \frac{L - 1/2}{4L^2 - 6L + 3}, \qquad L = \ln\left(\frac{R_{et}}{\Delta_t}\right) \tag{29}$$

$$M_{xt}^2 = M_{x\Delta t}^2 - 2M_{\theta et}^2 \ln\left(\frac{r_t}{\Delta_t}\right) \tag{30}$$

For $n = -0.5$,

$$M_{\theta et} = \sqrt{\frac{\lambda_t}{a}\phi\left(1 - \sqrt{1 - \frac{1}{L-2}\frac{M_{x\Delta t}^2 - 1}{b\phi}}\right)}$$

$$\phi = \frac{1}{2}\frac{L-2}{4\ln(L) - 6L + L^2}, \qquad L = \frac{R_{et}}{\Delta_t} \tag{31}$$

Otherwise ($n \ne -1$),

$$M_{\theta et} = \sqrt{\frac{\lambda_t}{a}\phi\left(1 - \sqrt{1 - \frac{n}{1 - Ln - L}\frac{M_{x\Delta t}^2 - 1}{b\phi}}\right)}$$

$$\phi = \frac{n}{2}\frac{1 - Ln - L}{(1+n)^2L^2 - (n+2)L + (1+n)/(1+2n)} \tag{32}$$

$$L = \left(\frac{\Delta_t}{R_{et}}\right)^{2n}$$

and for these last two cases,

$$M_{xt}^2 = M_{x\Delta t}^2 - M_{\theta et}^2\left(1 + \frac{1}{n}\right)\left[\left(\frac{r_t}{R_{et}}\right)^{2n} - L\right] \tag{33}$$

In the case of a free-vortex flow $n = -1$, the integral in Eq. (9) is equal to zero. Therefore, the axial Mach number in this case is constant. Approximate expressions for the tangential and axial Mach numbers at the nozzle throat for an exponential swirl type, $w = w_e\{(1 - \exp[-(r/r_0)]^2)/(1 - \exp[-(R_e/r_0)]^2)\}(R_e/r)$, are

$$M_{\theta et} = \sqrt{\frac{\lambda_t}{2ab}\frac{M_{xat}^2 - 1}{2(R_{et}/r_0)^2\left(\left\{Ei\left[1, 2(R_{et}/r_0)^2\right] - Ei\left[1, (R_{et}/r_0)^2\right] + \ln(2)\right\}\Big/\left\{1 - \exp\left[-(R_{et}/r_0)^2\right]\right\}^2\right) - 1}} \tag{34}$$

$$M_{xt}^2 = M_{xat}^2 - 2M_{\theta et}^2\left(\frac{R_{et}}{r_0}\right)^2\frac{Ei\left[1, 2(r/r_0)^2\right] - Ei\left[1, (r/r_0)^2\right] + \ln(2)}{\left\{1 - \exp\left[-(R_{et}/r_0)^2\right]\right\}^2}, \qquad Ei(n, x) = \int_1^\infty \frac{\exp(-x\cdot t)}{t^n}\,\mathrm{d}t \tag{35}$$

Because of the complexity of this case, the analytical treatment can be done only to a second-order approximation. [terms of the order $\mathcal{O}(M_{\theta et}^4)$ are neglected.] Then, Eqs. (8) and (9) were used to solve the distribution of the axial Mach number at the nozzle throat. For validation of the simplified analytical solution, a very accurate direct numerical solution was obtained as well, as is implied from the following scheme. The numerical procedure includes integration using the trapez method, whose accuracy depends on the integration step. The very fine grid used guarantees accuracy up to the seventh digit after the decimal point. The iterative solution of the integral equation used the interval halving method with a convergence criterion of a similar precision, 10^{-8}. Hence, for all practical applications, the numerical solutions may be considered "exact solutions" of the mathematical equations. Figures 2 and 3 show the very good agreement between the analytical approximations and the exact results (numerical solutions) for the tangential Mach number at the wall of the nozzle throat.

The swirl types were compared on the basis of the same swirl number S (Ref. 16) (Fig. 4):

$$S = \frac{\int_0^{R_e} \rho u w r^2\,\mathrm{d}r}{R_e \int_0^{R_e} \rho u^2 r\,\mathrm{d}r} \tag{36}$$

As a result of the swirl, the axial velocity profile changes, and its shape depends on the tangential velocity profile. Another interesting result is that the axial Mach number at the throat exceeds unity at a part of the cross section, in contrast to the nonswirling flow.[17]

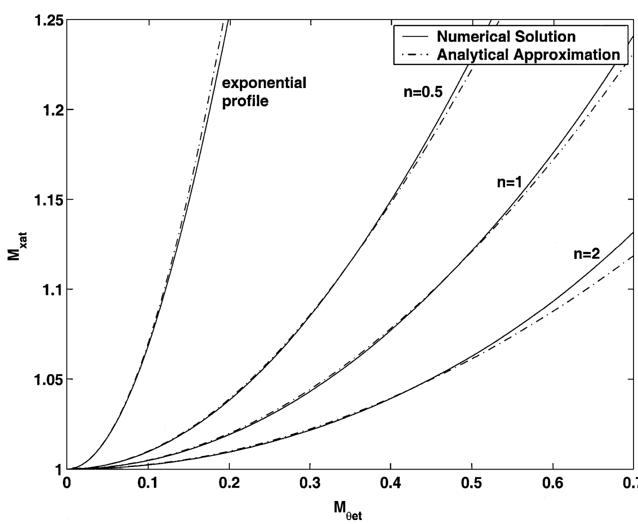

Fig. 2 Axial Mach number on the centerline vs tangential Mach number on the wall at nozzle throat for solid-body type and exponential swirl profiles.

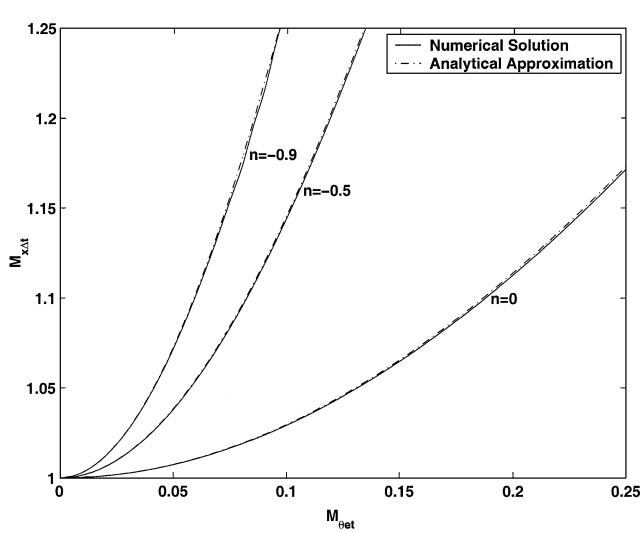

Fig. 3 Axial Mach number at $r = \Delta_t$ vs tangential Mach number on the wall at nozzle throat for free-vortex-type swirl profiles with $\Delta_t/R_{et} = 0.03$.

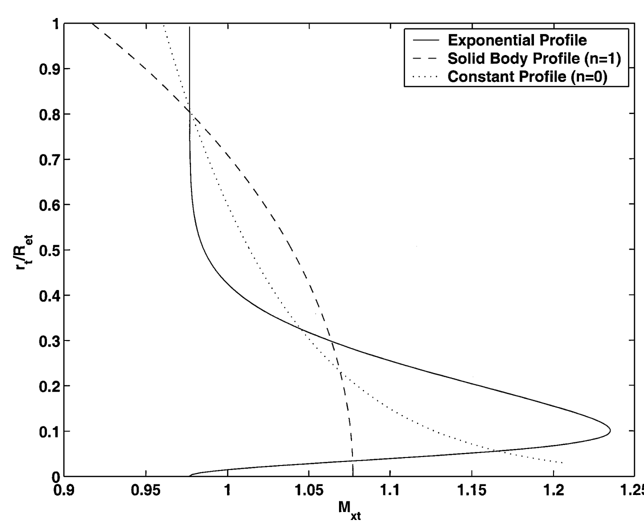

Fig. 4 Axial Mach number distribution at the nozzle throat for various swirl profiles, $S = 0.2$.

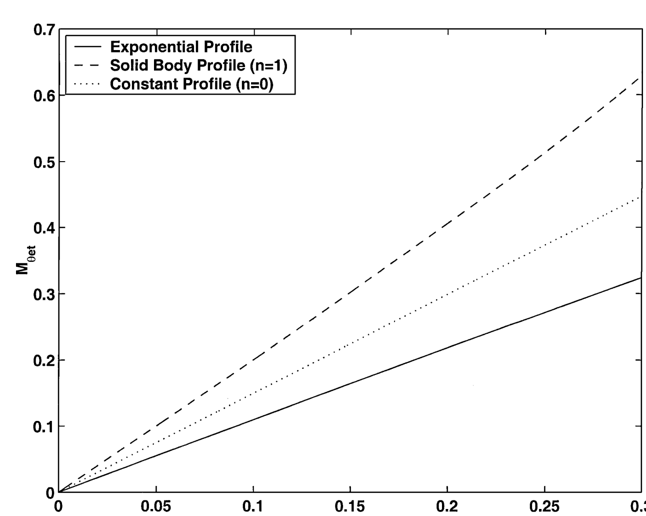

Fig. 5 Tangential Mach number at the nozzle throat wall vs swirl number for various profiles.

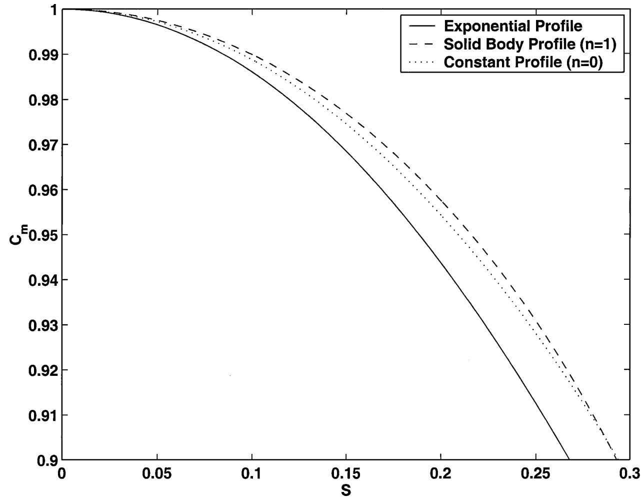

Fig. 6 Mass flux coefficient vs swirl number for various swirl profiles.

Figure 5 demonstrates the increase in the tangential Mach number at the nozzle throat wall as a result of increasing the swirl number S for different swirl types.

Figure 6 shows the decrease in the mass flow rate through the nozzle for the same stagnation pressure, as the swirl number increases. Note that under equal stagnation conditions, the relative mass flow rate is directly reflected by C_m.

IV. Conclusions

This work presents a new method to analyze choked swirling flows of a general tangential velocity distribution, introducing a choking criterion similar to the one used in one-dimensional nonswirling flows. One of the main outcomes of this work is the presentation of a simplified analytical solution procedure that is shown to yield very good approximations. The study reveals that, as a consequence of the tangential velocity, the axial Mach number distribution changes according to the swirl type and the mass flow rate through the nozzle decreases with swirl number.

References

[1]Mager, A., "Approximate Solution of Isentropic Swirling Flow Through a Nozzle," *ARS Journal*, Vol. 31, No. 8, 1961, pp. 1140–1148.

[2]King, W. S., "On Swirling Nozzle Flows," *Journal of Spacecraft and Rockets*, Vol. 4, No. 10, 1967, pp. 1404, 1405.

[3]Lewellen, W. S., Burns, W. J., and Strickland, H. J., "Transonic Swirling Flows," *AIAA Journal*, Vol. 7, No. 7, 1969, pp. 1290–1297.

[4]Gillespie, T. D., and Shearer, J. L., "The Control of Thrust and Flow Rate in Choked Nozzles by Vortex Generation," *Fluidics Quarterly*, 1972, pp. 50–55.

[5]Cutler, A. D., and Barnwell, R. W., "Vortex Flow in a Convergent–divergent Nozzle," *AIAA Journal*, Vol. 37, No. 10, 1999, pp. 1329–1331.

[6]Batson, J. L., and Sforzini, R. H., "Swirling Flow Through a Nozzle," *Journal of Spacecraft and Rockets*, Vol. 7, No. 2, 1970, pp. 159–163.

[7]Norton, D. J., Farquhar, B. W., and Hoffman, J. D., "An Analytical and Experimental Investigation of Swirling Flows in Nozzles," *AIAA Journal*, Vol. 7, No. 10, 1969, pp. 1992–2000.

[8]Marcum, D. L., and Hoffman, J. D., "Calculation of Three-Dimensional Inviscid Flowfields in Propulsive Nozzle with Center Bodies," *Journal of Propulsion and Power*, Vol. 4, No. 2, 1988, pp. 172–179.

[9]Smith, R., "An Investigation of Supersonic Swirling Jets," *Aeronautical Quarterly*, Vol. 24, 1973, pp. 167–178.

[10]Thompson, H. D., and Hoffman, J. D., "Swirling Flow in Thrust Nozzles," *Journal of Propulsion and Power*, Vol. 6, No. 2, 1990, pp. 151–157.

[11]Blatter, A., and Keranen, T. W., "A Vortex Valve for Flow Modulation of 5500°F Gas," *Journal of Spacecraft and Rockets*, Vol. 7, No. 2, 1970, pp. 169–174.

[12]Walsh, R. F., Lewellen, W. S., and Stickler, D. B., "A Solid Propellant Rocket Motor Modulated by a Fluidic Vortex Valve," *Journal of Spacecraft and Rockets*, Vol. 8, No. 1, 1971, pp. 77–79.

[13]Greenberg, I., and Wolff, H., "Cold Flow Evaluation of Parameters Influencing Thrust Modulation by a Fluidic Vortex Valve," *Israel Journal of Technology*, Vol. 13, No. 1, 1975, pp. 73–81.

[14]Natan, B., Gany, A., and Wolff, H., "Thrust Modulation of Solid Propellant Rockets by Means of a Fluidic Vortex Valve with Secondary Combustion," *Acta Astronautica*, Vol. 9, No. 12, 1982, pp. 703–711.

[15]Batchelor, G. K., *An Introduction to Fluid Dynamics*, Cambridge Univ. Press, London, 1979.

[16]Gupta, A. K., Lilley, D. G., and Syred, N., *Swirl Flows*, Abacus, Kent, England, U.K., 1985.

[17]Hsu, C. T., and DeJoode, A. D., "Inviscid Swirling Flows Through a Choked Nozzle," *AIAA Journal*, Vol. 11, No. 11, 1973, pp. 1564–1566.

M. Sichel
Associate Editor